Simulating wildfires with lab-heating experiments: Drivers and mechanisms of water repellency in alpine soils

Simulating wildfires with lab-heating experiments: drivers and mechanisms of water repellency in Alpine soils.

S. Negri*[1], S. Stanchi[1,2], L. Celi[1], E. Bonifacio[1]

[1]University of Torino, Department of Agricultural, Forest and Food Sciences, Largo Braccini 2, 10095 Grugliasco, Italy

[1]University of Torino, Natrisk, Interdepartmental Research Centre on Natural Risks in Mountain and Hilly Environments Largo Braccini 2, 10095 Grugliasco, Italy

*corresponding author

Keywords: hydrophobicity; Alps; soil burning; organic matter; soil minerals

Abstract

Wildfires induce deep modifications in soils. Water Repellency (WR) is one of the prime edaphic properties experiencing alterations upon heating. Despite occurrence, extent and persistence of burning-induced soil WR has been extensively discussed, the dynamics at the basis of its formation (and loss) are still widely unclear. The vast majority of research on this topic has been conducted in the Mediterranean area, even if alpine environments are far from being untouched by fires. Alpine soils are less developed than Mediterranean ones, and differ in mineralogy and composition of organic matter (and thereby present different interactions). We thus wanted to clarify some key mechanisms regulating WR thermal alterations in an understudied environment.

Our sampling design aimed at collecting soils representative of the Western Alps. Sample heating was performed in the lab at fixed temperatures (up to 300° C), on a set of A horizons developed under pine and beech forest covers. Water Drop Penetration Time (WDPT) and Sessile Drop Contact Angle (CA) were used to test WR. Soils were analyzed in terms of organic matter (OM), pH, serpentine relative abundance, texture and DCB-extractable iron (Fe).

WR was found to be extremely variable. Soils rich in OM, especially if containing abundant aromatic compounds, were found to be the most hydrophobic at room temperature. In samples exhibiting an increase in WR upon burning, repellency was maximized in correspondence of 200° C. WR was drastically lost when samples were heated at temperatures greater than 200° C. Above this threshold, pH systematically increased and the percentage of organic carbon (OC) sharply decreased. The change in pH is likely to have triggered an increase in the negative charge of mineral surfaces, resulting in a significant OM desorption and OC oxidation, eventually leading to a super-hydrophilic behavior in soil. The present investigation evidenced the susceptibility of Alpine soils towards thermal alteration, addressing the factors (organic matter composition and mineralogy) that mostly influence the hydrophobic behavior of these soils.

1. Introduction

Wildfires are ecosystem shapers (Pickett and White, 1985) that deeply alter canopy and litter cover, causing the redistribution of light and nutrients (Mataix-Solera and Cerdà, 2009). Fires affect a wide variety of chemical, physical and biological soil properties (Certini, 2005). High severity wildfires can heat soils up to 675° C, while temperatures below 450° and 250° C are experienced, respectively, during moderate and low fire intensities (Janzen and Tobin-Janzen, 2008). Usually, only the topsoil is actually heated by a fire due to low soil thermal conductivity (DeBano et al., 1998). Fuel type and duration of the event determine the degree of soil alterations (Robichaud, 2000), with changes in soil pH (Glaser et al., 2002), organic matter (OM) abundance and composition (Knicker, 2011; Merino et al., 2018), mineralogy (Araya et al., 2016; Reynard-Callanan et al., 2010), aggregate size and stability (Andreu et al., 2001; Mataix-Solera et al., 2011). The variations in soil properties concur in altering soil water repellency (WR) (Varela et al., 2010), one of the most important soil parameters generally evaluated after a wildfire (Plaza-Álvarez et al., 2018).

Water repellency causes a reduction in the water infiltration capacity of a soil and may be present even in unheated soils, at their natural state (Bisdom et al., 1993). Wildfires can trigger an increase in soil hydrophobicity (Malkinson and Wittenberg, 2011), as a greater WR can be found in soils experiencing high-

48 severity wildfires (Ferreira et al., 2005). A relevant role regarding soil WR has been attributed to OM
49 contents, composition and its interactions with the soil mineral phase (Atanassova and Doerr, 2010).
50 Aromaticity of OM increases with heat severity (Baldock and Smernik, 2002): during charring, aliphatic
51 hydrocarbons transform into polycyclic aromatic hydrocarbons (PAH) (Knicker, 2011). PAH migrate
52 downwards into the soil medium following a temperature gradient and condense as coatings on mineral
53 particles (DeBano, 2000). Resins, waxes and aromatic compounds are, among the charred organic residues,
54 responsible for an enhancement in hydrophobicity (Arcenegui et al., 2008). In addition, amphiphilic
55 compounds are able to cluster in micelles that, by exposing their hydrophobic moieties to the exterior,
56 shield the inner region from direct contact with water molecules (Wandruszka et al., 1999). The hydrophilic
57 head of amphiphilic compounds is usually bound to mineral hydroxylated surfaces by means of ligand-
58 exchange reactions (Tiberg et al., 1999),. As intense heating triggers OM volatilization (Knicker et al., 2006),
59 water repellent organic coatings are generally destroyed above 250° C (DeBano, 2000). Considering the
60 importance of OM composition in WR formation, a tight link exists between the type of vegetation (and
61 thus of litter) that undergoes burning and the degree of WR exhibited by the underlying soil. Evergreen
62 species have been appointed as able to trigger extreme WR, as shown by studies conducted on soils under
63 *Pinus pinaster* Aiton and *Pinus halepensis* Mill. burnt stands (Arcenegui et al., 2008).

64 The role played by the soil mineral phase should not be disregarded. It is widely accepted that coarse-
65 textured soils display a far greater WR because of a low surface area, consequently experiencing a more
66 efficient OM coating effect (Scott, 2000). Nevertheless, even clay-rich soils can give rise to extreme WR
67 upon burning (Doerr et al., 2000), either because heat leads to the cementation of small aggregates into
68 bigger ones (Bisdom et al., 1993) or because OM loadings are sufficient to cover the greater surface of
69 smaller-sized particles (Doerr et al., 1996). However, little is known about the effect of specific clay
70 minerals. WR was found to be inhibited in presence of kaolinite (Mataix-Solera et al., 2008), likely because
71 of the exposure of the hydrophilic octahedral sheet (Šolc et al., 2011). A similar WR inhibition was however
72 also observed in presence of Ca-montmorillonite (Dlapa et al., 2004). When dealing with factors affecting
73 soil WR, the abundance of soil iron (Fe) oxides and hydroxides should also be taken into consideration. Fe

74 minerals of great surface area, such as ferrihydrite (Cornell and Schwertmann, 2003), are commonly found
75 in topsoils and could directly trigger either a higher or lower wettability depending on the balance between
76 the larger surface area and the high affinity for OM sorption (Newcomb et al., 2017).

77 Deciphering the mechanisms involved in soil WR formation is of prime relevance. Most of the studies
78 dealing with WR have been conducted in Mediterranean environments (e.g. Arcenegui et al., 2008; Mataix-
79 Solera et al., 2008; Varela et al., 2010), even though Alpine ecosystems are far from being untouched by
80 fires and are extremely prone to runoff and erosion triggered by WR (Certini, 2005). The soils of the Alps
81 are different from the Mediterranean ones in terms of both OM and mineralogy. Kaolinite, for example, is
82 relatively common in areas with Mediterranean climates while it is mostly lacking in the Alps because of a
83 lower degree of soil development. Another T-O phyllosilicate, similar to kaolinite, is anyway often present
84 in alpine soils in relation to the occurrence of serpentinite rocks (Legros, 1992). Serpentinites are
85 metamorphic rocks mostly composed of serpentine, a group of 1:1 Mg layer silicates, with accessory
86 chlorites, talc, olivine, and pyroxenes, often in combination with magnetite and chromite (Moody, 1976).
87 Alpine soils developing on these rocks are poor in plant nutrients but contain high levels of Fe, Mg and
88 heavy metals like Ni and Cr (D'Amico et al., 2014). Serpentine, as kaolinite, possesses a low surface area
89 alongside with hydrophilic surfaces (Dixon et al., 1989). However, due to the presence of Mg in the
90 octahedral sheet, its hydrophilicity should be higher than that of kaolinite.

91 Laboratory-controlled heating experiments are widely adopted to mimic the behavior of different fire
92 typologies/intensities. Nevertheless, only a small portion of the existing studies aimed at targeting
93 transformations in superficial wettability in connection to heating-induced changes in OM and soil
94 mineralogical composition. Plus, none investigated the typical features of Alpine soils as, for example, the
95 role of serpentine in relation to soil wettability It yet has to be clarified whether this phyllosylicate acts as a
96 WR inhibitor (wettable tendency) or booster (low surface area)

97 Thus the aims of this paper ~~we~~are: i) to investigate the occurrence and evolution of heating-induced WR in
98 Alpine soils , and ii) to unravel the role of soil OM and mineral phases on natural and heating-induced WR.

2. Materials and methods

2.1. Study area, soil sampling and heating treatment

The study was conducted on a set of soils collected in two neighboring valleys located in Piedmont, North-Western Italy (see Supp. Info, Figure S.1) at elevations ranging from 1004 to 2037 m a.s.l. The whole area is characterized by a pre-alpine climate with average mean temperatures of about 6° C and annual precipitation that used to be 800 mm (IPLA, 2001; IPLA, 2000). A shift towards drier conditions was however observed by averaging the data of the last twenty years, with 630 mm of annual precipitation (http://webgis.arpa.piemonte.it/geoportale/). Both valleys belong to the geological Complex of Schists and Green stones, with the presence of different lithological formations like ophiolitic outcrops (amphibolites and serpentinites), calcschists and acid metamorphic rocks (micaceous schists and gneiss) (Servizio Geologico d'Italia, 2009). The samples were collected below two dominant forest types: European beech (BE series, 10 samples) and Scots pine (PI series, 8 samples) stands (Table 1). Soils of this area are mostly little developed and can thus be classified as Regosols and Cambisols, according to the WRB (IUSS Working Group WRB, 2014). The sampling sites were chosen to specifically fall in areas that did not experience burning in the last 10 years.

Soil sampling was performed by removing litter and organic horizons until the mineral soil surface was exposed, then the upper A horizon was collected. Soil samples were air-dried, sieved (2 mm) and stored at room temperature until laboratory analysis. Each sample was divided into six homogeneous subsamples. Ten g of each subsample were placed in aluminum cups with a base of 20 cm^2, resulting in samples with a thicknesss of less than 0.5 cm. One cup was kept at room temperature, while each of the others was oven heated for 30 minutes in a furnace equipped with a thermocouple at a specific temperature (T): 100°, 150°, 200°, 250° and 300° C. A heating time of 30 minutes was selected in accordance ~~to~~ with recent studies (Araya et al., 2017, 2016; Varela et al., 2010). Existing literature reported that loss of WR is generally experienced close to 250° C, therefore we selected such T values in order to mimic low-moderate fire intensities (Janzen and Tobin-Janzen, 2008) and be able to observe changes in WR.

2.2.Soil analyses

2.2.1. Soil Water Repellency estimation

Soil WR was evaluated by using both the Water Drop Penetration Time (WDPT) and the Sessile drop Contact Angle (CA) determination methods. The former was adopted for unheated and heated samples (at all T) to monitor the persistence of WR, while the latter was employed only in the case of unheated samples to estimate their initial and maximum hydrophobicity.

XXXXX. To ensure comparability of results, WDPT was evaluated after keeping the samples in a vacuum chamber for 30 minutes. Room relative humidity was verified to be always around 30-50 % during WDPT testing (Beatty and Smith, 2010; Diehl et al., 2010; Papierowska et al., 2018). We employed a standard 0.1 mŁ dropper to place 10 drops of distilled water on the soil flattened surface.

When water infiltration occurs, CA between the liquid and the gaseous phase (internal angle of the water drop) is ≤90° (Letey, 1969). CA was determined on 2 mm sieved soil samples (Bachmann et al., 2000; Papierowska et al., 2018). The soil was spread over a glass slide, pressed with a 100 g weight for about 5 s, and a drop of water (20 µL) was placed on the soil flattened surface. Measurements were performed in triplicate (Diehl et al., 2010). The placing of the water drops onto the soil surface was recorded with a 25x digital camera and the frame taken at the exact moment of water-soil contact was used for CA measurement. As CA tends to reduce with time (from contact, at time zero, to water penetration into the soil), we considered the maximum and most significant observable value (Beatty and Smith, 2010). A semi-automated procedure was implemented for CA determination. Each image was processed with MATLAB 2020a to highlight the boundaries of the drop. The Processing Toolbox was used for edge detection after gray scaling. The images were then imported in ImageJ and the Contact Angle Tool was employed. CA was calculated on the base of the ellipse-derived drop fitting (Diehl and Schaumann, 2007). Figure S.2 (see Supp. Info) displays two images of drops set on two different samples, with edge enhancement and ellipse-derived CA.

148 **2.2.2. Soil physical, chemical and mineralogical analyses**

149 Soil particle size distribution (PSD) was determined using the pipette method after dispersion with Na-
150 hexametaphosphate (Gee and Bauder, 1986). Size classes were classified as: coarse sand (2000-200 µm),
151 fine sand (200-50 µm), coarse silt (50-20 µm), fine silt (20-2 µm) and clay (<2 µm). Soil pH was evaluated in
152 a 1:2.5 soil:deionized water suspension after 2 h shaking (Procedures for Soil Analysis, 2002). Total C and N
153 were analyzed by dry combustion using a Unicube CHNS Analyzer (Elementar, Langenselbold, Hesse,
154 Germany). Carbonate content was determined volumetrically after HCl treatment (Nelson, 1982) and
155 inorganic C content was subtracted from total C to obtain organic carbon (OC) content. Pseudo-total Ni was
156 extracted with concentrated hot HNO_3-HCl digestion (Soil Survey Staff, 2014), followed by element
157 concentration determination by atomic absorption spectrometry, AAS (PerkinElmer AAnalyst 400, Norwalk,
158 CT, USA). Total Fe oxides were extracted using a sodium dithionite-citrate-bicarbonate (DCB) solution
159 (Mehra and Jackson, 1960) and Fe content was determined by AAS. Specific Surface Area (SSA, $m^2 g^{-1}$) was
160 quantified by performing the methylene blue stain test (Chiappone et al., 2004).

161 Clay was separated by sedimentation after dispersion with Na-hexametaphosphate, flocculated with $MgCl_2$,
162 washed until free of chloride and freeze-dried. The abundance of serpentine was assessed on air-dried
163 oriented mounts by X-ray diffraction (XRD), using a Philips PW 1710 diffractometer (40 kV, 20 mA, CoKα
164 radiation and graphite monochromator). Scans were made from 3 to 35° 2θ at a speed of 1° 2θ min^{-1}, the
165 background was subtracted and the peak intensities and positions were obtained using PowderX software.
166 An index of abundance of serpentine (SRPH, from 0 to 1) was obtained as the ratio of the height of the *001*
167 serpentine peak at 0.73 nm to the sum of the heights of all identified layer silicates, as fully described
168 elsewhere (Bonifacio et al., 2010).
169 The determination of pH, OC, N were performed not only at room temperature, but also on lab heated
170 samples at all temperatures.

171 Soil OM composition of samples BE4, BE10, PI5 and PI7 was investigated by means of Fourier Transform-
172 Infrared (FT-IR) spectroscopy. These samples were selected to represent the variability of the dataset in
173 terms of canopy cover (BE and PI), lithology (BE4 and PI7 on schist, BE 10 and PI5 on serpentinite) and WR

behavior. Potassium bromide (KBr) pellets were prepared by adding 4 mg of soil sample to 400 mg of KBr, thoroughly ground and mixed. KBr was oven-dried prior to use so as to avoid water absorption. FT-IR spectra were acquired (PerkinElmer Spectrum 100, Norwalk, CT, USA) in the 4000–450 cm^{-1} region, with a resolution of 4 cm^{-1}. Sixteen scans per sample were obtained, with KBr pellet as background. PerkinElmer IR WinLab Spectrum software was used to process the spectra, performing baseline correction and normalization. The same software was also employed to perform semi-quantitative analysis, calculating the intensity and area corresponding to some selected bands.

2.3.Statistical analyses

RStudio (R version 4.0.2) was used for all the statistical analyses. Normality and homoscedasticity of the data were checked before comparisons between groups by, respectively, Shapiro-Wilk's and Levene's tests. Non-normal data were log-scaled. One-way ANOVA was used to detect differences in mean values between groups, setting the threshold for statistical significance at the level of 0.05. Tukey-HSD test was applied for post hoc pairwise comparisons. Linear mixed models (LMM) were implemented when investigating trends, so as to verify the role played by selected covariates along a T-controlled kinetic (25°-300° C). Autocorrelation, when present, was considered within the model structure and the best fitting model was chosen on the basis of Akaike's information criterion (AIC). Correlation matrices were computed with the use of the non-parametric rank-based Spearman method as part of the data was non-linear. Clustering was operated by building an Euclidean distance matrix, selecting Ward's agglomeration method and then performing dendrogram pruning. The validity of the parameters related to height (y-axis) and number of desired clusters was verified by the application of PERMANOVA test to the obtained clusters. When a p-value lower than 0.05 was obtained, the clustering was assumed as optimal. Principal Component Analysis (PCA) was applied to investigate the relationship between relevant variables. Matrices adopted for PCA were scaled and centered prior to performing the analysis and generating biplots.

3. Results

3.1.Soil properties at natural state and WR

All samples fell in the textural classes of loamy sand and sandy loam soils, with a mean total sand content of 71 % (st. dev=6 %) (Table 2). Coarse sand (mean=45 %, st. dev=10 %) always prevailed over fine sand (mean=26 %, st. dev=9 %). The abundance of coarse fractions was reflected by relatively low SSA values (mean=11.7 $m^2 g^{-1}$, st. dev=5.8 $m^2 g^{-1}$). Only one sample (PI7) displayed SSA values over 20 $m^2 g^{-1}$, probably due to its high clay content. SSA resulted slightly but significantly correlated with clay ($R=0.501$, $p<0.05$), OC ($R=0.540$, $p<0.05$) and N ($R=0.640$, $p<0.01$) contents. The horizons of the BE series~~collected under beech canopy cover~~ were generally characterized by a greater acidity ($p<0.001$) than the soils of the PI ~~pine~~ subset. Nickel content and SRPH were consistent and in agreement ($R=0.659$, $p<0.05$) in highlighting those horizons with opposite bedrock-derived nature, despite Ni contents were not homogeneously distributed among the samples. The PI ~~pine~~ subset, in fact, presented overall lower Ni values with respect to the ~~beech subset~~ BE series ($p<0.05$), probably due to a lithological inheritance. Nevertheless, samples BE2, BE6, BE7, BE9, BE10, PI5 and PI6 presented extremely high SRPH values and considerable Ni contents and could be unequivocally addressed as serpentine soils. OC and N values were lower in BE samples with respect to PI samples ($p<0.01$ and $p<0.05$, respectively). The lowest OC contents were found in samples BE5 and BE6 (less than 20 g kg^{-1} OC). C/N ratio was slightly, but not significantly, higher in the PI series ~~samples~~ with respect to the BE series ~~samples~~. DCB-extractable Fe (mean=15.2 g kg^{-1}, st. dev=4.9 g kg^{-1}) was overall but not significantly ($p>0.05$) higher in the BE subset ~~under beech canopy cover~~.

Figure 1 displays the FT-IR spectra at 25° C of the selected soil samples. The spectra of both BE and PI samples displayed a large band in the 3700-3000 cm^{-1} region mainly due to O-H/N-H stretching of OM compounds, although also O-H from hydration water and octahedral layer of serpentine can contribute to the intensity of that band, especially close to 3700-3600 cm^{-1} (Russell, 1987). C-H stretching of aliphatic compounds (2940 cm^{-1}) was little visible and did not vary much among the samples. In the 1650-1500 cm^{-1} region, the most pronounced bands due to C-C stretching of aromatic structures were observed in soils of

the PI series ~~samples~~. This mirrors the difference in OM composition that distinguishes the two forest cover types (tree species). The large band observed in the 1000 cm^{-1} region (lowest in BE10), generally attributed to C-O stretching of alcoholic groups, is here masked by Si-O and Me-O groups.

Water repellency measured by WDPT and CA on unheated samples is visible in Figure 2. The complete infiltration time ranged from <1 to 9 s in the BE subset and from 4 to over 120 s in the PI soil series. The analyzed soil samples thus displayed a WR behavior ascribable to the categories of wettable (0-5 s), slightly hydrophobic (5-60 s) and moderately hydrophobic (60-600 s) (Bisdom et al., 1993). CA values did not exceed 120° in both sets, the maximum CA value obtainable for a sphere placed on a planar surface. In comparison, the BE subset displayed less variations in WDPT than in CA. Above 90°, which is the CA threshold value assumed for the occurrence of water infiltration, soil samples clearly displayed two different behaviors. A linear trend could be observed when measuring wettability (WDPT vs CA) in the ~~beech~~ BE subset ($R=0.922$ $p<0.001$), while an exponential trend emerged for the PI subset ~~pine~~ ($R=0.894$, $p<0.001$) (Figure 2).

Infiltration time (WDPT) was found to be directly related to OC ($R=0.839$, $p<0.0001$) and N ($R=0.706$, $p<0.001$) contents. Similar relationships were obtained considering CA as WR estimator ($R=0.789$, $p<0.0001$ and $R=0.767$, $p<0.001$, respectively). No other strong and straightforward relationship emerged between WR measurements and soil properties.

3.2.Heating-induced changes in soil properties and WR

After heating, the soils displayed a large variability in WDPT, both in the BE and in the PI subsets (Figure 3). Regardless of the species of belonging, not all samples showed an increase in WR upon burning. In the horizons showing greater infiltration times with increasing heat intensities, WDPT peaked in correspondence of 200° C. The highest WDPT values of the BE subset were lower than those of the PI series, as here extremely high infiltration times were recorded (e.g. over 3500 s in PI1). A drastic drop in infiltration times occurred with temperatures higher than 200° C (Figure 3), regardless of the behavior displayed by the samples at lower temperatures.

Samples were clustered according to their T-dependent WR behavior (WDPT at all T) within each subset (Figure 4). In the ~~beech~~ BE subset (Figure 4a) the clustering originated three significantly different groups ($p<0.001$) while the ~~pine~~ PI subset (Figure 4b) resulted evidently divided into two groups ($p<0.05$). In the BE subset (Figure 4a), the clustering procedure well isolated the most wettable samples (BE4, BE5, BE6; cluster BE III), which displayed significantly lower infiltration times already at room-temperature ($p<0.001$). The clustering further divided the samples displaying an increase in burning induced WR (BE1, BE7 and BE9; cluster BE I), from those with stationary WR values (cluster BE II). In the ~~pine~~ PI subset (Figure 4b), this tendency was even more expressed. Cluster PI I included only the soils with extreme WR at 200° C. Already at room-temperature, WDPT values of these samples were significantly higher than those of cluster PI II ($p<0.01$).

The pH (Figure 5a) was, within each species-specific series (BE and PI), significantly lower in more repellent soil clusters ($p<0.001$) while OC and N contents (Figure 5b & 5c) were, at the same time, significantly higher ($p<0.001$ for both). In all the samples, pH remained stationary until 200° C (Figure 5a) then it systematically increased. A similar stationary trend was visible also in organic C contents, which drastically dropped above 200° C (Figure 5b). Total N contents displayed only small variations, occurring mostly in the ~~pine~~ PI subset (Figure 5c). Differences in C and pH trends were found to be statistically significant in terms of T ($p<0.001$ for both). At 300° C, OC content was significantly lower than at less intense Ts, while pH was significantly higher. The combined effect of T and cluster of belonging (T:cluster interaction) was not significant ($p>0.05$ for both). The percentage of OC loss at 300° C, with respect to the initial OC value, was not significantly greater in different species or clusters ($p>0.05$). Below 250° C, WR dependency upon OC and N contents was found to be altered by temperature. A strong positive correlation remained between WDPT and OC contents, but the strength of the relationship systematically decreased upon heating ($R=0.913$, $p<0.001$ at 100°, $R=0.891$, $p<0.001$ at 150°, $R=0.713$, $p<0.001$ at 200° C). The same happened in the case of WDPT and N, with a less pronounced magnitude ($R=0.691$, $p<0.01$ at 100°, $R=0.624$, $p<0.01$ at 150°, $R=0.463$, $p<0.05$ at 200° C). No direct link between the C/N ratio and WDPT could be evinced, as the cluster with less hydrophobic soils had a lower C/N value (Figure S.3b), but without any statistical significance ($p>0.05$).

Upon increasing temperature, the FT-IR spectra became more and more featureless (Figure 6a). The greatest changes in intensity were appreciated in the regions corresponding to O-H/N-H and C-H groups (3500 to 2900 cm^{-1}) and C-C, C-O (1650-1500 cm^{-1}) of OM. No heat-mediated variation occurred in correspondence of 3700-3600 cm^{-1}, which suggests that O-H groups visible in that region mostly belong to soil minerals and became more isolated with growing T (especially in BE4, PI7 and PI5). Figure 6b shows the ratio between the peak area at 3500-2900 cm^{-1} to the peak area at 3700-3600 cm^{-1} (that did not change upon heating). No evident modifications occurred in the 3500-2900 cm^{-1} band up to 200° C, if not a slight reduction in samples BE4 and PI5. A sharp reduction took place at 300° C in all the samples, indicating that most of O-H and C-H groups of OM were affected at this temperature. Figure 6c displays the ratio between the peak area at 1650-1500 cm^{-1} to the peak area at 3700-3600 cm^{-1},. Also in this case heating up to 200° C did not cause significant changes, if not a slight increase in the 1650-1500 cm^{-1} region in BE10 and PI7, likely due to an enrichment of aromatic moieties. When reaching 300° C, all the soils lost the greatest part of functional groups in this region (C-C, C-O of aromatic compounds). The greatest loss can be observed in the BE subset, especially in the case of the least hydrophobic and OM poorest of the selected samples (BE4). PI soil samples were slightly less affected, especially the most WR and OM richest (PI5).

Soil clusters containing samples with a greater WR tendency, within each species-specific subset (namely cl. BE I and cl. PI I), were enriched in serpentine (Figure S.3c, Supp. Info) and DCB-extractable Fe (Figure S.3d), but the differences were not statistically significant ($p>0.05$ for both).

The main soil parameters involved in WR formation at 200° C, T at which hydrophobic behavior was maximum, were employed to depict two PCA objects, one for each soil series (BE and PI, Figure 7a & 7b). The explained variance accounted for more than 60 % in both cases (71 % BE series, 68 % PI series). In Figure 7a, BE subset, PC1 was intimately tied to the abundance of either sand or silt and DCB-extractable Fe. PC2 was instead related on one extreme to higher contents of clay and on the other extreme to greater contributions of OC and SRPH. In Figure 7b, PI soil series, PC1 was mostly ruled by PSD (sand on one side, silt and clay on the other), while PC2 was tied to DCB-extractable Fe and OC contents. The difference

existing between clusters PI II and PI I seems to be related to the abundance of fine fractions, whereas, for BE samples, cluster BE III (most wettable behavior) was oriented towards lower C and greater clay contents.

4. Discussion

Heating-induced WR was found to be significantly tied to room-temperature WR in A horizons of Alpine soils. Regardless of the vegetation cover type (pine or beech forests), T-mediated hydrophobicity build-up occurred in soils that displayed the least wettable behavior already at 25° C, in agreement with the literature (Atanassova and Doerr, 2011). These samples maximized WR at 200° C. Conversely, other samples did not exhibit any increase in WR with growing temperatures, with low and stationary infiltration times. Regardless of the WR behavior displayed until 200° C, all WR was lost above that temperature.

4.1. What regulates room-temperature soil WR?

Unheated samples of the PI subset resulted moderately hydrophobic, while the majority of soils in the BE subset ~~samples~~ were wettable, according to the classification by Bisdom et al. (1993). The two methods employed for WR estimation (WDPT and CA) were in agreement with each other, as found by Papierowska et al. (2018), but the relationship existing between them differed in the two soil series (BE vs PI, Figure 2). WDPT and CA were linearly related in the BE subset, while the relationship was exponential in the PI soil series. CA addresses the initial repellency of a soil, while WDPT does not give an estimate of the actual degree of hydrophobicity but rather deals with the persistence of WR (Diehl, 2013). Thus, samples of the ~~pine~~ PI subset, despite falling in the same CA range of beech specimens, exhibited a far greater persistence of repellency.

Organic carbon content (significantly higher in the PI series) was found to be the dominant factor regulating room-temperature WR in the analyzed poorly developed alpine soils. The relationship between the degree of soil WR and OM abundance was sometimes found to be positive (Mao et al., 2014), sometimes negative (Teramura, 1980) and sometimes nonexistent (de Blas et al., 2010). Some authors mention the existence of an OC saturation threshold in correspondence of which the addition of extra OM does not induce a greater

hydrophobicity in soil (Doerr et al., 2000). In our case, no evidence suggesting OM surface saturation was observable, despite the high OC contents (up to 97 g kg^{-1}). Not only WR was found to be strongly related to the amounts of organic C, but its dependency upon OM composition stood out as well. Considering the two species separately, in fact, the relationship between WR and OC resulted stronger in the ~~case of~~ the BE subset ~~soil samples~~ ($R=0.867$, $p<0.001$ for CA, $R=0.927$, $p<0.001$ for WDPT) ~~with~~ with respect to the PI subset ~~soil samples~~ ($R=0.643$, $p<0.05$ for CA, $R=0.548$, $p<0.05$ for WDPT). This implies that in presence of more hydrophobic OM, testified by the greater amount of aromatic compounds in the PI samples (Figure 6c), a weaker correlation between WR and OC contents exists. Conversely, when OM is characterized by a lower degree of intrinsic hydrophobicity (BE series ~~soil samples~~, with less predominance of aromatic compounds), a greater dependency upon OC loadings occurs. Aromatic compounds might easily interact with uncharged mineral surfaces (like those of quartz and other primary minerals) via hydrophobic forces (Oudou and Hansen, 2002). The coarsest soil fractions, mainly composed of inherited minerals in alpine soils, could therefore not only trigger a greater WR because of a low surface area but they could also potentially offer surfaces with a high affinity for hydrophobic organic molecules. The relationship between WR and soil properties may therefore result as highly complex and multifaceted, especially in the case of pine.

4.2.What regulates heating-induced WR evolution?

The heat-induced increase in WR in the analyzed soil samples was not linear and not homogeneous alongside the T kinetic, and the highest WDPT values were recorded at 200° C (Figure 3). The soil clusters (three in the BE subset, two in the PI subset) differed in several soil characteristics that may actually explain their wettability tendencies. Soils with the most repellent behavior (those that experienced heat-induced WR build-up) presented higher OC contents (Figure 7, Figure S.3a) and, within their species-specific subset, they were also enriched in DCB-extractable Fe and serpentine in the clay fraction (Figure 7a & 7b, Figure S.3d & S.3c). OM tends to bind weakly with serpentine surfaces (Falsone et al., 2016) but their coating could nonetheless enhance WR, as this phyllosilicate has a low surface area. Furthermore, even hydrophilic mineral surfaces can develop hydrophobic properties when covered with low O/C humic acids (Murphy et

al., 1990). As we analyzed A horizons, the soil mineral surfaces were certainly already partially coated by organic compounds at different degrees of transformation. On the other hand, DCB-extractable Fe abundance in more repellent samples might imply a larger extent of high-affinity surfaces that, once experiencing OM coating, could induce a greater WR. A preferential adsorption of reactive aromatic compounds was reported on Fe oxy-hydroxides (Chassé et al., 2015; Newcomb et al., 2017). It seems therefore plausible to hypothesize that an extremely, if not the most, hydrophobic fraction of OM tends to adhere on the surface of oxides. As framed by the PCAs at 200° C, nevertheless, factors regulating WR did not act in the same way in the two analyzed soil series. The BE subset (Figure 7a) presented the least repellent soil cluster in correspondence of greater amounts of clay together with low OC and SRPH contents. In the PI soil subset (Figure 7b) DCB-extractable Fe and OC were oriented in the same direction, but the two WR clusters mainly differed in terms of PSD (sand vs silt and clay abundance). The relatively hydrophilic PI7, for example, was not actually poor in OM (OC=69 g kg^{-1}) but presented the highest amount of clay in the whole dataset (Table 1). As expected, a greater WR is generally experienced by coarse-textured soils (DeBano, 1991; Doerr et al., 2000; Scott, 2000), with low clay contents (Harper et al., 2000). In this context, anyway, not all factors controlling WR remained unaltered in the investigated T range. The change in the relationship between WR and OC from 25° to 200° C (decreasing strength of the correlations WDPT vs OC and CA vs OC) could imply that, with growing temperatures, not only OM quantity but also T-induced changes in OM quality determine the degree of WR experienced by a soil. Burning has different effects on OM, primarily depending on the nature of the source material, together with charring intensity and oxygen availability (Knicker, 2007). The frequently reported increase in OM aromaticity (Baldock and Smernik, 2002; Knicker, 2011) seems to be the key factor inducing a more efficient coating of mineral particles, thus hindering a greater WR. The observation of functional groups by FT-IR spectroscopy revealed that a small reduction in surface hydroxyl groups and aliphatic compounds (3500-2900 cm^{-1}) occurred already at 200° C (Figure 6b). Conversely, aromatic compounds (C-C, C-O stretching at 1650-1500 cm^{-1}, Figure 6c) were well represented and even slightly more present. The wide variety of WR behaviors

373 displayed by these soils could ultimately be linked also to OM patchy distribution on mineral surfaces
374 (Kaiser and Guggenberger, 2003).

375 Up to 200° C, the pH remained mostly unchanged (Figure 5a). WR is reported to be maximum when soils
376 remain in the range of their natural pH (Graber et al., 2009). In addition, a greater repellency is usually
377 observed for soils with low pH values. As the pKa of carboxylic acids falls in the pH range of 3-5 (Diehl et al.,
378 2010), a reduction in repulsion forces between these groups may cause micelle-like aggregation with
379 outward-oriented hydrophobic moieties (Duval et al., 2005; Terashima et al., 2004). Figure 5a in fact
380 displays that, within each species-specific subset, the most repellent group had lower pH values.

381 4.3.What causes WR loss above 200° C?

382 Literature reports a temperature threshold of more than 250° C above which WR is lost by the destruction
383 of organic compounds responsible for the coating of mineral surfaces (DeBano, 2000). In some studies (e.g.
384 Mataix-Solera et al., 2008), Mediterranean soils heated up to 350° C for 20 minutes still displayed a
385 distinctive WR behavior (more than 2000 s of infiltration time). In our case, for alpine soils, WR disappeared
386 already just above 200° C, when a sharp reduction in OC was visible (Figure 5b). A decrease in OC is
387 generally observed starting from 220° C (Giovannini et al., 1988), but the greatest OC losses are usually
388 experienced between 250° and 450° C (Araya et al., 2017, 2016) for a greater volatilization triggered by
389 intense heating (Knicker, 2011). A larger sensitivity towards thermal alteration of OM in high elevation
390 forest soils was observed also in other environments, even in case of moderate heating temperatures
391 (Santos et al., 2016). Burning soils above 200° C caused here a neat flattening of the FT-IR spectra (Figure
392 6). However, not all the organic compounds were affected to the same extent. The areas corresponding to
393 stretching of O-H/N-H and C-H (Figure 6b) and C-C,C-O (Figure 6c) groups decreased in all the analyzed
394 samples from 200° to 300° C. Other studies observed a reduction in C-H stretching (2950-2850 cm^{-1}),
395 corresponding to aliphatic groups (Šimkovic et al., 2008) and a significant decrease in O-H stretching peaks
396 (3700-3000 cm^{-1}) occurring around 250° C (Araya et al., 2017). The persisting peak in correspondence of
397 3700-3600 cm^{-1} (Figure 6) was attributed to O-H of soil 1:1 clay minerals like serpentine (Russell, 1987).

Nitrogen, on the contrary, did not show any systematically decreasing trend (Figure 3c), but indeed N greatest loss, for combustion and volatilization, generally occurs only above 350° C (Araya et al., 2017). However, OC loss is not likely the sole responsible for the dramatic decrease of WR observed in the transition from 200° to 250° C, as the samples of the most hydrophobic cluster, cl. PI I, were still rich in OM at 250° C (more than 50 g kg^{-1} OC, Figure 5b). Thus, in order to understand what is inducing a hydrophilic behavior in soil, we need to consider the alterations occurring in the mineral phase and how these modifications influence bonds with OM. The layer silicate structure is generally not affected by temperatures around 250°-300° C, while haematite formation from goethite is reported to occur close to 250° C (Brown, 1980). Also, thermal transformations of ferrihydrite typically require temperatures of at least 300° C, depending on the amounts of incorporated Si or metals (Jambor and Dutrizac, 1998). The surface area of haematite is generally much lower than that of ferrihydrite (32 vs 245 $m^2 g^{-1}$) (Kaiser and Guggenberger, 2003; Celi et al., 2020), therefore these thermal modifications should induce a more efficient OM coating of mineral surfaces, giving rise to a greater WR. Nevertheless, the sorption capacity of mineral surfaces and the interactions with the organic compounds may experience changes by the increase in pH visible above 200° C (Figure 5a). This phenomenon could be attributed to proton consuming decarboxylation reactions and release of base cations from organic matter (Badìa and Martì, 2003). As aforementioned, out-ward orienting of hydrophobic moieties in amphiphilic micelles occurs only at relatively low pH values (Duval et al., 2005; Terashima et al., 2004). As pH increases, a change in OM conformation may lead to more charged and elonged structures. A systematic increase in pH can in parallel trigger a more negative surface charge of soil mineral surfaces, especially where 1:1 phyllosilicates dominate (Diehl et al., 2010). OM sorption to mineral phases would thus be heavily affected because of the increased electrostatic repulsion between highly negatively charged surfaces (Mayer and Xing, 2001). It is indeed likely that, above 200° C, the remaining OM could be partially desorbed due to the increased negative charges. This would increase the fraction of mineral surfaces that become OM-free and available for interaction with water molecules, leading to the complete loss of WR.

5. Conclusions

~~We investigated heating-induced changes in WR in soil horizons representative of the degree of alteration and parent material characterizing the Western Alps, under two forest covers that are widespread on alpine reliefs. The results evidenced that~~ Soil OM quantity and quality were the main drivers of hydrophobicity at room-temperature in soil horizons representative of the degree of alteration and parent material characterizing the Western Alps. Upon growing T, the soil samples displayed extremely different wettable behaviors, with or without T-induced WR build-up. This happened mainly in relation to content and composition of OM, particle size distribution and abundance of serpentine and DCB-extractable Fe-oxides. WR was maximized at 200° C and dramatically lost above this T, regardless of the hydrophobicity displayed by samples at lower temperatures. The loss of WR was mainly attributed to heat-induced increase in the negative surface charge of mineral surfaces, linked to a systematic pH increase above 200° C. The drastic change in the surface charge of minerals might be able to inhibit, to some extent, OM sorption to mineral particles. By exposing a greater portion of OM-free surfaces, soil particles would thus be available for the interaction with water molecules, eventually leading to a super-hydrophilic behavior in soil. What clearly emerged, nonetheless, is that alpine soils experience the disruption of repellent organic coatings at lower T respect to other environments, possibly because of a different mechanism of OM retention on mineral phases, caused by specific litter composition and soil mineralogy.

The alpine environment is not unfamiliar to wildfire occurrence, thus a good comprehension of the mechanisms triggered by heating in soils is needed, especially considering that major changes in soil WR behavior were detected already at low-moderate fire intensities. Identifying the dynamics regulating wildfire-related WR is a crucial step to tackle the issue of ecosystem recovery. Addressing this matter is fundamental, considering that climate-change-related alterations in wildfires regimes are already causing the occurrence of more frequent and disruptive fires.

Acknowledgements

We would like to thank Sara Trevisani, Msc student, for having performed part of the analyses. The current research was funded by the University of Torino, “Fondo di ricerca locale 2019”.

References

Andreu, V., Imeson, A.C., Rubio, J.L., 2001. Temporal changes in soil aggregates and water erosion after a wildfire in a Mediterranean pine forest. Catena 44, 69–84.

Araya, S.N., Fogel, M.L., Berhe, A.A., 2017. Thermal alteration of soil organic matter properties: a systematic study to infer response of Sierra Nevada climosequence soils to forest fires. Soil 3, 31-44.

Araya, S.N., Meding, M., Berhe, A.A., 2016. Thermal alteration of soil physico-chemical properties: a systematic study to infer response of Sierra Nevada climosequence soils to forest fires. Soil 2, 351–366.

Arcenegui, V., Mataix-Solera, J., Guerrero, C., Zornoza, R., Mataix-Beneyto, J., García-Orenes, F., 2008. Immediate effects of wildfires on water repellency and aggregate stability in Mediterranean calcareous soils. Catena 74, 219–226.

Atanassova, I., Doerr, S.H., 2010. Organic compounds of different extractability in total solvent extracts from soils of contrasting water repellency. Eur. J. Soil Sci. 61, 298–313.

Atanassova, I., Doerr, S.H., 2011. Changes in soil organic compound composition associated with heat-induced increases in soil water repellency. Eur. J. Soil Sci. 62, 516–532.

Bachmann, J., Horton, R., Van Der Ploeg, R.R., Woche, S., 2000. Modified sessile drop method for assessing initial soil--water contact angle of sandy soil. Soil Sci. Soc. Am. J. 64, 564–567.

Badía, D., Martí, C., 2003. Plant ash and heat intensity effects on chemicaland physical properties of two contrasting soils. Arid L. Res. Manag. 17, 23–41.

468 Baldock, J.A., Smernik, R.J., 2002. Chemical composition and bioavailability of thermally altered *Pinus*
469 *resinosa* (Red pine) wood. Org. Geochem. 33, 1093–1109.

470 Beatty, S.M., Smith, J.E., 2010. Fractional wettability and contact angle dynamics in burned water repellent
471 soils. J. Hydrol. 391, 97–108.

472 Bisdom, E.B.A., Dekker, L.W., Schoute, J.F.T., 1993. Water repellency of sieve fractions from sandy soils and
473 relationships with organic material and soil structure. Geoderma 56, 105–118.

474 Bonifacio, E., Falsone, G., Piazza, S., 2010. Linking Ni and Cr concentrations to soil mineralogy: does it help
475 to assess metal contamination when the natural background is high? J. Soils Sediments 10, 1475–
476 1486.

477 Brown, G., 1980. Associated minerals, in: Brindley, G. W. & Brown, G. (Eds.) Crystal structures of clay
478 minerals and their X-ray identification. London Mineralogical Society, pp. 361–410.

479 Celi, L., Prati, M., Magnacca, G., Santoro, V., Martin, M., 2020. Role of crystalline iron oxides on stabilization
480 of inositol phosphates in soil. Geoderma, 374, 114442.

481 Certini, G., 2005. Effects of fire on properties of forest soils: a review. Oecologia 143, 1–10.

482 Chassé, A.W., Ohno, T., Higgins, S.R., Amirbahman, A., Yildirim, N., Parr, T.B., 2015. Chemical force
483 spectroscopy evidence supporting the layer-by-layer model of organic matter binding to iron (oxy)
484 hydroxide mineral surfaces. Environ. Sci. Technol. 49, 9733–9741.

485 Chiappone, A., Marello, S., Scavia, C., Setti, M., 2004. Clay mineral characterization through the methylene
486 blue test: comparison with other experimental techniques and applications of the method. Can.
487 Geotech. J. 41, 1168–1178.

488 Cornell, R. M, Schwertmann, U., 2003. The iron oxides : structure, properties, reactions, occurrences, and
489 uses, second ed. Weinheim: Wiley-VCH.

490 D'Amico, M.E., Bonifacio, E., Zanini, E., 2014. Relationships between serpentine soils and vegetation in a

491 xeric inner-Alpine environment. Plant Soil 376, 111–128.

492 de Blas, E., Rodríguez-Alleres, M., Almendros, G., 2010. Speciation of lipid and humic fractions in soils under
493 pine and eucalyptus forest in northwest Spain and its effect on water repellency. Geoderma 155, 242–
494 248.

495 DeBano, L.F., 2000. The role of fire and soil heating on water repellency in wildland environments: a review.
496 J. Hydrol. 231, 195–206.

497 DeBano, L.F., 1991. The effect of fire on soil properties, in: Proceedings Management and Productivity of
498 Western-Montane. Forest Soils. 151–155.

499 DeBano, L.F., Neary, D.G., Ffolliott, P.F., 1998. Fire effects on ecosystems. John Wiley & Sons, New York.

500 Diehl, D., 2013. Soil water repellency: Dynamics of heterogeneous surfaces. Colloids and Surfaces A:
501 Physicochem. Eng. Asp. 432, 8–18.

502 Diehl, D., Bayer, J. V, Woche, S.K., Bryant, R., Doerr, S.H., Schaumann, G.E., 2010. Reaction of soil water
503 repellency to artificially induced changes in soil pH. Geoderma 158, 375–384.

504 Diehl, D., Schaumann, G.E., 2007. The nature of wetting on urban soil samples: wetting kinetics and
505 evaporation assessed from sessile drop shape. Hydrol. Process. 21, 2255–2265.

506 Dixon, J.B., 1989. Kaolin and Serpentine Group Minerals, in: Dixon, J.B., Weed, S.B. (Eds.), Minerals in soil
507 environments. Soil Science Society of America, Madison, Wisconsin, pp. 467–525.

508 Dlapa, P., Doerr, S.H., Lichner, L., Sir, M., Tesar, M., 2004. Effect of kaolinite and Ca-montmorillonite on the
509 alleviation of soil water repellency. Plant Soil Environ. 50, 358–363.

510 Doerr, S.H., Shakesby, R.A., Walsh, R.P.D., 2000. Soil water repellency : its causes , characteristics and
511 hydro-geomorphological significance. Earth-Science Rev. 51, 33-65

512 Doerr, S.H., Shakesby, R.A., Walsh, R.P.D., 1996. Soil hydrophobicity variations with depth and particle size

513 fraction in burned and unburned *Eucalyptus globulus* and *Pinus pinaster* forest terrain in the Agueda
514 Basin, Portugal. Catena 27, 25–47.

515 Duval, J.F.L., Wilkinson, K.J., van Leeuwen, H.P., Buffle, J., 2005. Humic substances are soft and permeable:
516 evidence from their electrophoretic mobilities. Environ. Sci. Technol. 39, 6435–6445.

517 Falsone, G., Celi, L., Stanchi, S., Bonifacio, E., 2016. Relative importance of mineralogy and organic matter
518 characteristics on macroaggregate and colloid dynamics in Mg-silicate dominated soils. L. Degrad.
519 Dev. 27, 1700–1708.

520 Ferreira, A.J.D., Coelho, C.O.A., Boulet, A.K., Leighton-Boyce, G., Keizer, J.J., Ritsema, C.J., 2005. Influence of
521 burning intensity on water repellency and hydrological processes at forest and shrub sites in Portugal.
522 Soil Res. 43, 327–336.

523 Gee, G.W., Bauder, J.W., 1986. Particle-size Analysis. In: Klute, A. (Ed.), Methods of Soil Analysis, Part 1,
524 second ed. Agronomy Monograph 9. Agron. Soc. of America and Soil Sc. Soc. of America, Madison,
525 Wisconsin, pp. 383–409.

526 Giovannini, G., Lucchesi, S., Giachetti, M., 1988. Effect of heating on some physical and chemical
527 parameters related to soil aggregation and erodibility. Soil Sci. 146, 255–261.

528 Glaser, B., Lehmann, J., Zech, W., 2002. Ameliorating physical and chemical properties of highly weathered
529 soils in the tropics with charcoal--a review. Biol. Fertil. soils 35, 219–230.

530 Graber, E.R., Tagger, S., Wallach, R., 2009. Role of divalent fatty acid salts in soil water repellency. Soil Sci.
531 Soc. Am. J. 73, 541–549.

532 Harper, R.J., McKissock, I., Gilkes, R.J., Carter, D.J., Blackwell, P.S., 2000. A multivariate framework for
533 interpreting the effects of soil properties, soil management and landuse on water repellency. J.
534 Hydrol. 231, 371–383.

535 IPLA, 2001. Piano Forestale Territoriale. Area forestale: Val Chisone e Germanasca. Reg. Piemonte.

536 http://www.sistemapiemonte.it/montagna/sifor/dwd/relazioni/AF26_rel_p1.pdf

537 IPLA, 2000. Piano Forestale Territoriale. Area forestale: Alta Valle Susa. Reg. Piemonte.
538 http://www.sistemapiemonte.it/montagna/sifor/dwd/relazioni/af30_rel_p1.pdf

539 IUSS Working Group WRB, 2014. World reference base for soil resources 2014. International soil
540 classification system for naming soils and creating legends for soil maps. Rome: FAO. World Soil
541 Resources Reports No. 106.

542 Jambor, J.L., Dutrizac, J.E., 1998. Occurrence and constitution of natural and synthetic ferrihydrite, a
543 widespread iron oxyhydroxide. Chem. Rev. 98, 2549–2586.

544 Janzen, C., Tobin-Janzen, T., 2008. Microbial Communities in Fire-Affected Soils, in: Dion P., Nautiyal C.S.
545 (Eds.) Microbiology of Extreme Soils. Soil Biology, vol 13. Springer, Berlin, Heidelberg, pp. 299-316.

546 Kaiser, K., Guggenberger, G., 2003. Mineral surfaces and soil organic matter. Eur. J. Soil Sci. 54, 219–236.

547 Kleber, M., Sollins, P., Sutton, R., 2007. A conceptual model of organo-mineral interactions in soils: self-
548 assembly of organic molecular fragments into zonal structures on mineral surfaces. Biogeochemistry
549 85, 9–24.

550 Knicker, H., 2011. Pyrogenic organic matter in soil: Its origin and occurrence, its chemistry and survival in
551 soil environments. Quat. Int. 243, 251–263.

552 Knicker, H., 2007. How does fire affect the nature and stability of soil organic nitrogen and carbon? A
553 review. Biogeochemistry 85, 91–118.

554 Knicker, H., Almendros, G., González-Vila, F.J., González-Pérez, J.A., Polvillo, O., 2006. Characteristic
555 alterations of quantity and quality of soil organic matter caused by forest fires in continental
556 Mediterranean ecosystems: a solid-state ^{13}C NMR study. Eur. J. Soil Sci. 57, 558–569.

557 Legros, J.P., 1992. Soils of Alpine mountains, in: Martini, I.P., Chesworth, W. (Eds.), Developments in Earth
558 Surface Processes, vol. 2, chapt. 7, Elsevier, pp. 155-181.

559 Letey, J., 1969. Measurement of contact angle, water drop penetration time, and critical surface tension.
560 Proc. Symp. Water Rep. Soils, Univ. Calif., Riverside, 43–47.

561 Malkinson, D., Wittenberg, L., 2011. Post fire induced soil water repellency — Modeling short and long-
562 term processes. Geomorphology 125, 186–192.

563 Mao, J., Nierop, K.G.J., Damsté, J.S.S., Dekker, S.C., 2014. Roots induce stronger soil water repellency than
564 leaf waxes. Geoderma 232, 328–340.

565 Mataix-Solera, J., Arcenegui, V., Guerrero, C., Jordán, M.M., Dlapa, P., Tessler, N., Wittenberg, L., 2008. Can
566 terra rossa become water repellent by burning? A laboratory approach. Geoderma 147, 178–184.

567 Mataix-Solera, J., Cerdà, A., 2009. 1.1Incendios forestales en España. Ecosistemas terrestres y suelos, in:
568 Cerdà, A.,Mataix-Solera, J. (Eds.), Efectos de los incendios forestales sobre los suelos en España, pp.
569 25-53

570 Mataix-Solera, J., Cerdà, A., Arcenegui, V., Jordán, A., Zavala, L.M., 2011. Fire effects on soil aggregation: a
571 review. Earth-Science Rev. 109, 44–60.

572 Mayer, L.M., Xing, B., 2001. Organic matter--surface area relationships in acid soils. Soil Sci. Soc. Am. J. 65,
573 250–258.

574 Mehra, O.P., Jackson, M.L., 1960. Iron Oxide Removal from Soils and Clay by a Dithionite-Citrate System
575 Buffered with Sodium Bicarbonate. Clays and Clay Minerals 7, 317-327.

576 Merino, A., Fonturbel, M.T., Fernández, C., Chávez-Vergara, B., García-Oliva, F., Vega, J.A., 2018. Inferring
577 changes in soil organic matter in post-wildfire soil burn severity levels in a temperate climate. Sci.
578 Total Environ. 627, 622–632.

579 Moody, J.B., 1976. Serpentinization: a review. Lithos 9, 125-138.

580 Murphy, E.M., Zachara, J.M., Smith, S.C., 1990. Influence of mineral-bound humic substances on the
581 sorption of hydrophobic organic compounds. Environ. Sci. Technol. 24, 1507–1516.

582 Nelson, R.E., 1982. Carbonate and gypsum, in: Methods Soil Anal. Amer Soc. Agronomy, Inc. Madison,
583 Winsconsin, pp. 181–196.

584 Newcomb, C.J., Qafoku, N.P., Grate, J.W., Bailey, V.L., De Yoreo, J.J., 2017. Developing a molecular picture
585 of soil organic matter--mineral interactions by quantifying organo--mineral binding. Nat. Commun. 8,
586 1–8.

587 Oudou, H.C., Hansen, H.C.B., 2002. Sorption of lambda-cyhalothrin, cypermethrin, deltamethrin and
588 fenvalerate to quartz, corundum, kaolinite and montmorillonite. Chemosphere 49, 1285–1294.

589 Papierowska, E., Matysiak, W., Szatyłowicz, J., Debaene, G., Urbanek, E., Kalisz, B., Łachacz, A., 2018.
590 Compatibility of methods used for soil water repellency determination for organic and organo-mineral
591 soils. Geoderma 314, 221–231.

592 Pickett, S.T.A., White, P.S., 1985. The ecology of natural disturbance and patch dynamics. Academic Press,
593 New York.

594 Plaza-Álvarez, P.A., Lucas-Borja, M.E., Sagra, J., Moya, D., Alfaro-Sánchez, R., González-Romero, J., las Heras,
595 J., 2018. Changes in soil water repellency after prescribed burnings in three different Mediterranean
596 forest ecosystems. Sci. Total Environ. 644, 247–255.

597 Procedures for Soil analysis, 2002. In: Van Reeuwijk L. P., WRB 2002, Technical Paper n. 9. International Soil
598 Reference and Information Centre, Wageningen, The Netherlands.

599 Reynard-Callanan, J.R., Pope, G.A., Gorring, M.L., Feng, H., 2010. Effects of high-intensity forest fires on soil
600 clay mineralogy. Phys. Geogr. 31, 407–422.

601 Robichaud, P.R., 2000. Fire effects on infiltration rates after prescribed fire in Northern Rocky Mountain
602 forests, USA. J. Hydrol. 231, 220–229.

603 Russell, J.D., 1987. Infrared methods, in: A Handbook of Determinative Methods in Clay Mineralogy. Wilson,
604 M. J. (Ed.), Chapman and Hall, pp. 133-171.

605 Santos, F., Russell, D., Berhe, A.A., 2016. Thermal alteration of water extractable organic matter in
606 climosequence soils from the Sierra Nevada, California. J. Geophys. Res. Biogeosciences 121, 2877–
607 2885.

608 Scott, D.F., 2000. Soil wettability in forested catchments in South Africa; as measured by different methods
609 and as affected by vegetation cover and soil characteristics. J. Hydrol. 231, 87–104.

610 Servizio Geologico d'Italia, 2009. Carta geologica d'Italia 1:50000, Regione Piemonte, Direzione Regionale
611 Servizi Tecnici e di Prevenzione.

612 Šimkovic, I., Dlapa, P., Doerr, S.H., Mataix-Solera, J., Sasinkova, V., 2008. Thermal destruction of soil water
613 repellency and associated changes to soil organic matter as observed by FTIR spectroscopy. Catena
614 74, 205–211.

615 Šolc, R., Gerzabek, M.H., Lischka, H., Tunega, D., 2011. Wettability of kaolinite (001) surfaces—molecular
616 dynamic study. Geoderma 169, 47–54.

617 Soil Survey Staff, 2014. Kellogg Soil Survey Laboratory Methods Manual. Soil Survey Investigations Report
618 No. 42, Version 5.0. R. Burt and Soil Survey Staff (Ed.). U.S. Department of Agriculture, Natural
619 Resources Conservation Service.

620 Teramura, A.H., 1980. Relationships between stand age and water repellency of chaparral soils. Bull. Torrey
621 Bot. Club 42–46.

622 Terashima, M., Fukushima, M., Tanaka, S., 2004. Influence of pH on the surface activity of humic acid:
623 micelle-like aggregate formation and interfacial adsorption. Colloids Surfaces A Physicochem. Eng.
624 Asp. 247, 77–83.

625 Tiberg, F., Brinck, J., Grant, L., 1999. Adsorption and surface-induced self-assembly of surfactants at the
626 solid--aqueous interface. Curr. Opin. Colloid Interface Sci. 4, 411–419.

627 Varela, M.E., Benito, E., Keizer, J.J., 2010. Effects of wildfire and laboratory heating on soil aggregate

628 stability of pine forests in Galicia: The role of lithology, soil organic matter content and water
629 repellency. Catena 83, 127–134.

630 Wandruszka, R. von, Engebreatson, R.R., Yates III, L.M., 1999. Humic acid pseudomicelles in dilute aqueous
631 solution: fluorescence and surface tension measurements. Underst. humic Subst. Adv. methods, Prop.
632 Appl. 79–85.

633 Zavala, L.M., Granged, A.J.P., Jordán, A., Bárcenas-Moreno, G., 2010. Effect of burning temperature on
634 water repellency and aggregate stability in forest soils under laboratory conditions. Geoderma 158,
635 366–374.

636

637

Figure captions

Figure 1: FT-IR spectra of bulk soil samples BE4, BE10, PI7 and PI5.

Figure 2: Correlation between WDPT (s) and CA (°) in the two datasets. Shaded area indicates standard deviation.

Figure 3: Average WDPT (s) measurements and standard deviation in a) ~~beech~~ BE subset and b) ~~pine~~ PI subset. Y axis in log scale.

Figure 4: Normalized WDPT values with deriving dendrograms, pruning lines and clusters for a) ~~beech~~ BE~~,~~ subset and b) ~~pine~~ PI subset.

Figure 5: Heating-induced changes in a) pH, b) OC and c) N. Samples are colored by cluster (mean and st. dev.)

Figure 6: a) FT-IR spectra of the selected samples (BE4, BE10, PI7 and PI5) with increasing T (25°-200°-300° C). Absorbance at 1200-1000 cm^{-1} was cut to better focus on the bands at 3500-2900 cm^{-1} and 1650-1500 cm^{-1}; b) Ratio of band areas (3500-2900) / (3700-3600) cm^{-1} for all the selected samples at all T; c) Ratio of band areas (1650-1500) / (3700-3600) cm^{-1} for all the selected samples at all T.

Figure 7: PCA with selected soil properties at 200° C with samples colored according to WR cluster in a) ~~beech~~ BE subset and b) ~~pine~~ PI subset.

Tables

Table 1: Main site characteristics of the selected soils. X and Y coordinates are in ED50/UTM Zone 32N format.

ID	X	Y	Elevation (m a.s.l.)	Forest type	Forest structure and cover	Dominant lithology
BE1	355856	5000989	1310	*Fagus sylvatica* L.	Coppice, presence of *Pinus sylvestris* L.	Gneiss
BE2	356071	5001254	1300	*Fagus sylvatica* L.	High forest, presence of *Pinus sylvestris* L. and *Betula pendula* Roth.	Serpentinite
BE3	356552	5001406	1100	*Fagus sylvatica* L.	High forest	Micaschist
BE4	361810	4998612	1350	*Fagus sylvatica* L.	Coppice, mixed with other broadleaves	Micaschist
BE5	361898	4998600	1350	*Fagus sylvatica* L.	Coppice, mixed with other broadleaves	Micaschist
BE6	361557	4999206	1180	*Fagus sylvatica* L.	Coppice	Serpentinite
BE7	361481	4999762	1250	*Fagus sylvatica* L.	Coppice, mixed with other broadleaves	Serpentinite
BE8	361671	4999535	1300	*Fagus sylvatica* L.	High Forest	Chloritoidschist
BE9	370948	4997803	1300	*Fagus sylvatica* L.	Coppice, presence of *Pinus sylvestris* L.	Serpentinite
BE10	370923	4997399	1300	*Fagus sylvatica* L.	High Forest	Serpentinite
PI1	351268	4987287	1004	*Pinus sylvestris* L.	Mixed with *Quercus spp*. and *Castanea sativa* Mill.	Gneiss and metagranite
PI2	343419	4989449	1336	*Pinus sylvestris* L.	Mixed with *Larix decidua* Mill.	Calcschist
PI3	336948	4984292	1570	*Pinus sylvestris* L.	Mixed with *Larix decidua* Mill.	Micaschist
PI4	333889	4980778	2037	*Pinus sylvestris* L.	Mixed with *Larix decidua* Mill.	Mica schist
PI5	329440	4977921	1560	*Pinus sylvestris* L.	Mixed with *Larix decidua* Mill.	Serpentinite
PI6	326280	4978275	1360	*Pinus sylvestris* L.	Pure, sparse	Serpentinite
PI7	324940	4979413	1510	*Pinus sylvestris* L.	Mixed with *Larix decidua* Mill.	Micaschist
PI8	333257	4991623	1031	*Pinus sylvestris* L.	Pure, dense	Colluvium – mixed lithology

658 **Table 2: Main soil properties of the analyzed soil samples. Letters for statistically significant mean values (group**

659 **series, BE vs PI) are reported below.**

ID	Coarse Sand (%)	Fine Sand (%)	Coarse Silt (%)	Fine Silt (%)	Clay (%)	SSA (m^2g^{-1})	SRPH	pH	OC ($g\ kg^{-1}$)	N ($g\ kg^{-1}$)	C/N	Ni ($mg\ kg^{-1}$)	Fe DCB ($g\ kg^{-1}$)
BE1	42	26	12	16	4	5.9	0.12	4.4	40.5	2.8	14.5	560	16.5
BE2	43	34	8	12	3	11.8	0.52	4.8	34.7	2.3	15.1	1468	16.6
BE3	26	44	9	17	5	8.0	0.24	6.8	41.2	2.6	15.8	456	19.4
BE4	38	33	11	15	4	9.2	0.13	5.7	31.3	2.8	11.2	258	13.8
BE5	41	36	7	12	5	8.0	0.08	5.1	14.2	1.6	8.9	207	16.4
BE6	40	24	9	21	6	8.4	0.46	6.0	13.2	1.8	7.3	974	17.8
BE7	54	21	7	15	4	5.9	0.63	4.0	42.3	3.7	11.4	1718	21.0
BE8	33	38	14	13	3	19.3	0.17	4.9	42.0	3.4	12.4	358	18.3
BE9	35	29	13	19	4	16.8	0.60	5.5	67.5	4.8	14.1	1285	19.0
BE10	57	17	8	14	3	10.5	0.78	4.5	39.7	3.3	12.0	1704	9.7
PI1	54	23	9	9	5	13.4	0.28	6.6	64.3	4.0	16.1	279	25.6
PI2	50	23	6	16	6	5.0	0.19	7.9	30.9	2.3	13.5	116	9.7
PI3	54	19	9	13	5	15.1	0.14	6.2	97.1	7.0	13.9	96	12.9
PI4	41	22	11	22	5	16.4	0.27	5.9	53.8	4.5	12.0	120	18.2
PI5	59	19	7	11	4	15.5	0.89	6.5	76.2	6.4	11.9	571	10.0
PI6	63	10	5	16	7	14.3	0.57	7.1	54.7	3.4	16.1	583	9.6
PI7	41	18	9	22	10	24.8	0.24	7.1	69.3	5.0	13.9	337	9.1
PI8	41	36	15	7	1	2.1	0.34	7.7	54.2	2.3	23.6	37	9.5
BE mean	41^b	30^a	10	15	4	10.4	0.37	5.2^b	36.7^b	2.9^b	12.3	899^a	16.8
BE std	9	8	2	3	1	4.5	0.25	0.8	15.4	0.9	2.7	605	3.2
PI mean	50^a	21^b	9	14	5	13.3	0.37	6.9^a	62.6^a	4.4^a	15.1	267^b	13.1
PI std	9	7	3	6	2	7.0	0.25	0.7	19.4	1.7	3.8	215	5.9

660

661

662 **Figures**

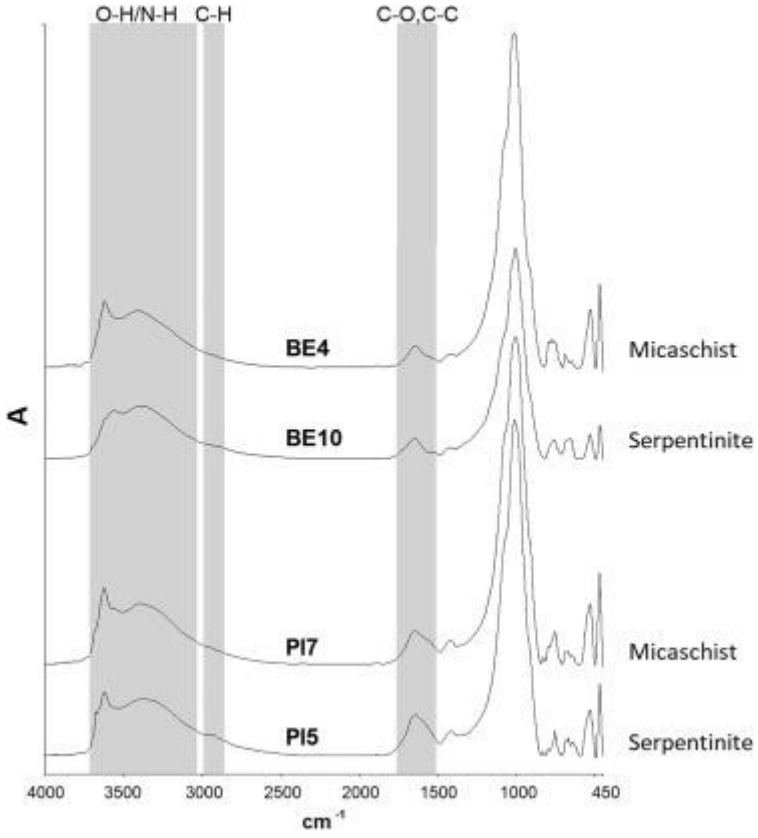
O-H/N-H
C-H
C-O,C-C
A
BE4
Micaschist
BE10
Serpentinite
PI7
Micaschist
PI5
Serpentinite
4000
3500
3000
2500
2000
1500
1000
450
cm-1

663

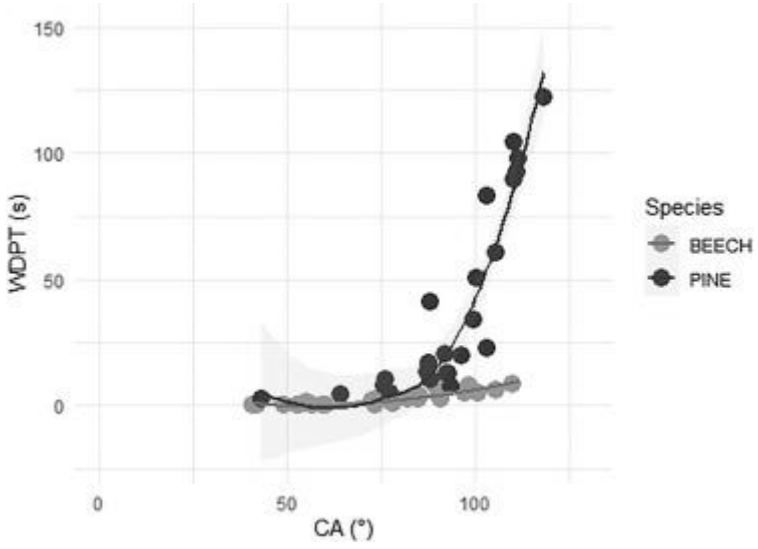
150
100
50
0
WDPT (s)
0
50
100
CA (°)
Species
BEECH
PINE

664

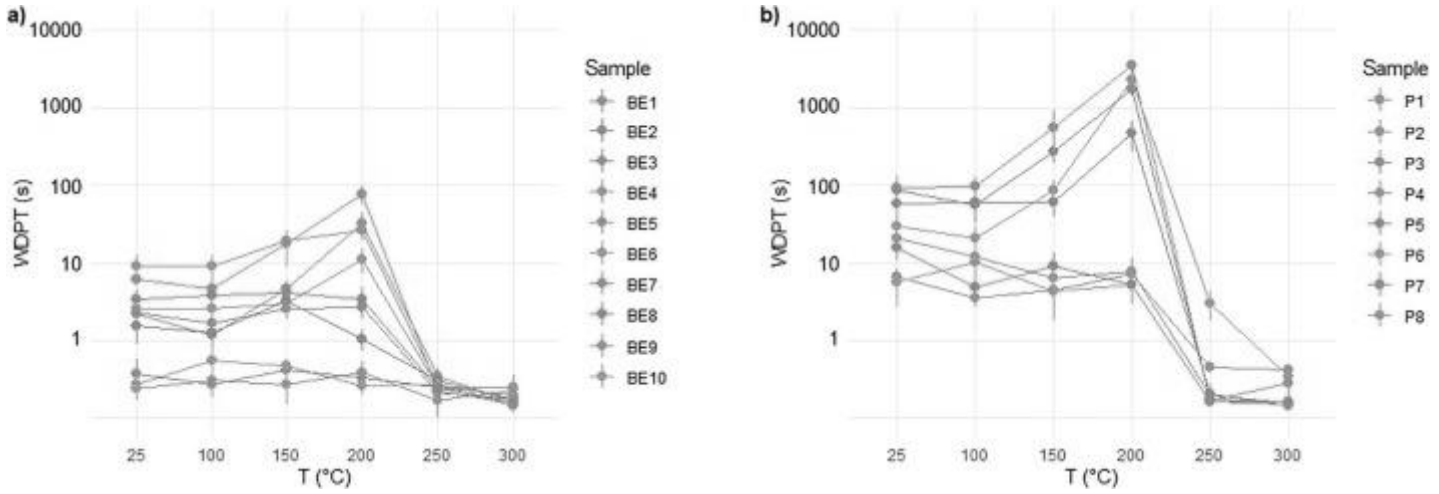

665

666

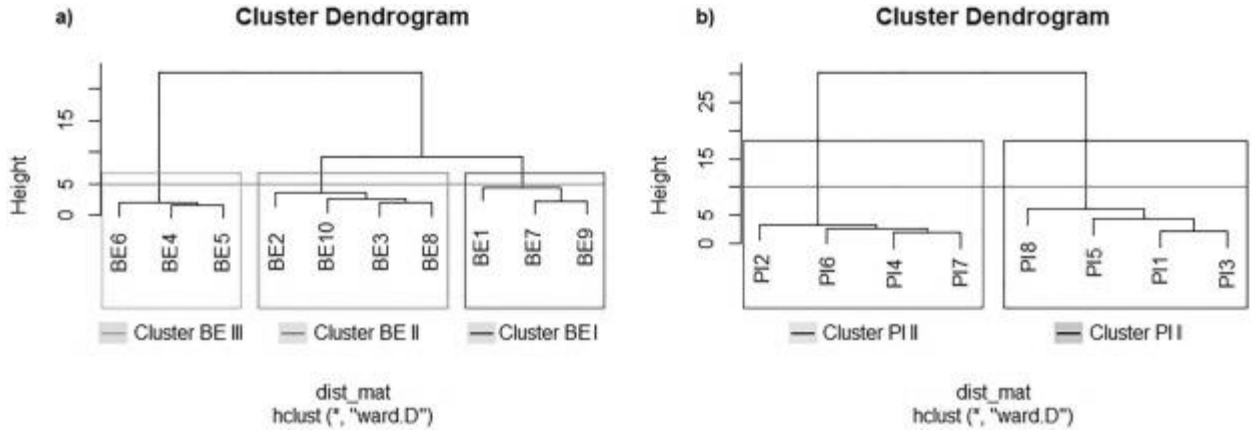

667

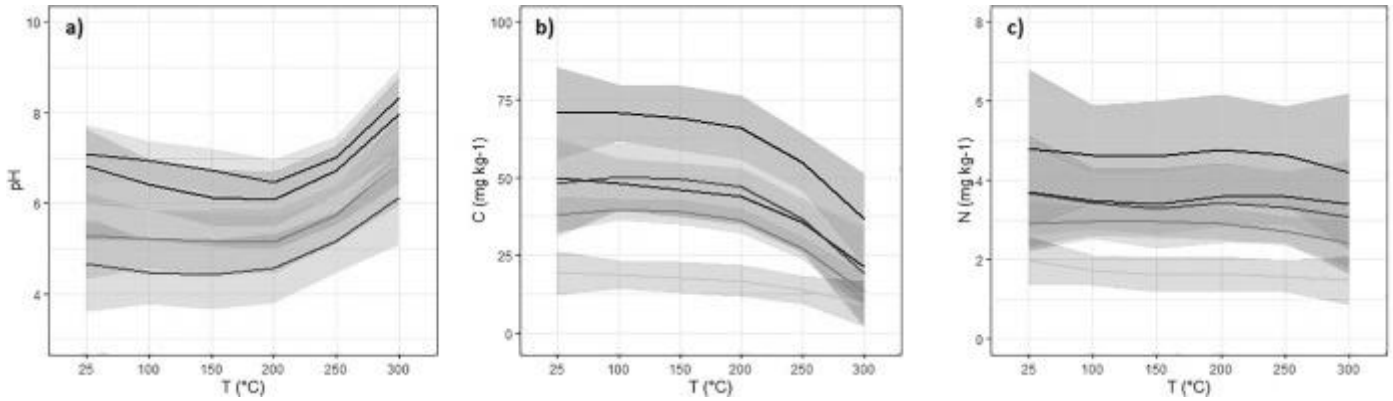

668